NASA TECHNICAL NOTE

NASA TN D-6648
c. 1

NASA TN D-6648

RANDOM WALK STUDY OF ELECTRON MOTION IN HELIUM IN CROSSED ELECTROMAGNETIC FIELDS

by Gerald W. Englert

Lewis Research Center
Cleveland, Ohio 44135

NATIONAL AERONAUTICS AND SPACE ADMINISTRATION • WASHINGTON, D. C. • FEBRUARY 1972

1. Report No. NASA TN D-6648	2. Government Accession No.	
4. Title and Subtitle RANDOM WALK STUDY OF ELECTRON MOTION IN HELIUM IN CROSSED ELECTROMAGNETIC FIELDS		5. Report Date February 1972 6. Performing Organization Code
7. Author(s) Gerald W. Englert		8. Performing Organization Report No. E-6453
9. Performing Organization Name and Address Lewis Research Center National Aeronautics and Space Administration Cleveland, Ohio 44135		10. Work Unit No. 112-02 11. Contract or Grant No.
12. Sponsoring Agency Name and Address National Aeronautics and Space Administration Washington, D. C. 20546		13. Type of Report and Period Covered Technical Note 14. Sponsoring Agency Code
15. Supplementary Notes		

16. Abstract

Random walk theory, previously adapted to electron motion in the presence of an electric field, is extended to include a transverse magnetic field. In principle, the random walk approach avoids mathematical complexity and concomitant simplifying assumptions and permits determination of energy distributions and transport coefficients within the accuracy of available collisional cross section data. Application is made to a weakly ionized helium gas. Time of relaxation of electron energy distribution, determined by the random walk, is described by simple expressions based on energy exchange between the electron and an effective electric field. The restrictive effect of the magnetic field on electron motion, which increases the required number of collisions per walk to reach a terminal steady state condition, as well as the effect of the magnetic field on electron transport coefficients and mean energy can be quite adequately described by expressions involving only the Hall parameter.

17. Key Words (Suggested by Author(s))

Random walk
Plasma
Electric discharge
Gaseous discharge
Electron transport coefficients

18. Distribution Statement

Unclassified - unlimited

19. Security Classif. (of this report)	20. Security Classif. (of this page)	21. No. of Pages	22. Price*
Unclassified	Unclassified	36	$3.00

* For sale by the National Technical Information Service, Springfield, Virginia 22151

RANDOM WALK STUDY OF ELECTRON MOTION IN HELIUM IN CROSSED ELECTROMAGNETIC FIELDS

by Gerald W. Englert

Lewis Research Center

SUMMARY

Random walk theory, previously adapted to electron motion in the presence of an electric field, is extended herein to include a transverse magnetic field. Application is made to a weakly ionized helium gas. Interactions of the electrons with the helium atoms are based on integral and differential experimental cross section data. Electronic excitations and ionizations as well as elastic collisions are included. Electron trajectories between collisions are based on exact solution of the equations of motion for a Lorentz gas.

The restrictive effect of the magnetic field on electron motion increases the number of collisions per walk required for an assembly of electrons in an arbitrary initial distribution to relax to a terminal steady state condition. This limits the maximum value of the ratio of magnetic field strength B to background pressure p possible to study with reasonable computer time. A range of B/p from 2.25×10^{-5} to 2.25×10^{-4} weber per newton (30 to 300 G/torr) was investigated. This covers the range of a very weak to a very strong influence of B/p on electron transport coefficients.

Time of relaxation of electron energy distribution, determined by random walks, is approximated by a simple expression based on energy exchange between the electrons and the electric field. The influence of the magnetic field is to effectively reduce the ratio of electric field to background pressure by $\sqrt{1 + (\omega\tau)^2}$ (where ω and τ^{-1} are the cyclotron and collision frequencies, respectively).

Electron transport coefficients as well as energy and velocity distributions were determined and compared with existing theory. Effect of the magnetic field on mean energy and transport coefficients is in most cases predicted within 10 percent of the random walk results by use of the Hall parameter $\omega\tau$. The constant mean free time and the isotropic scattering approximation often used in analytical studies, are accurate within the scatter of the data (estimated to less than 5 percent).

INTRODUCTION

Study of electron motion in an electric field has been actively pursued for three-quarters of a century (refs. 1 and 2). It was, in fact, investigation of the cathode rays of the gaseous discharge which led to the discovery of the electron (ref. 3). The random walk concept, first formulated in 1905 (ref. 4), contributed significantly to descriptions of stochastic particle motions as present in such gaseous conductors. Except in the simplest cases (refs. 5 and 6), these descriptions lead to hard-to-solve differential equations (ref. 5). On the other hand, calculation of random walks step by step permits, in principle, inclusion of much physical detail with little mathematical complexity. Such random walks have very seldom been performed; apparently because of the burdensome repetitious task of calculating the motions of statistically representative numbers of test particles throughout an enormous number of steps.

Appearing first in the literature is the manual effort of Yarnold (ref. 7) to determine an electron energy distribution at low electric field strength. With electron-molecule energy exchange in mind, a low mass ratio M/m of 100 was used in an effort to reduce the number of operations (collisions) required in the walks. Later, with the aid of a computer, Wannier (ref. 8) calculated the walk of one ion for 10 000 steps, yielding the relatively easy to determine drift and diffusion motion. Some approximate ion velocity distributions were attempted. Only elastic collisions were considered. Relatively large samples of test particles and/or numbers of steps per walk are required to find detailed electron energy distributions when inelastic losses such as electronic excitation and ionization are considered. It is especially laborious to determine the Townsend first ionization coefficient at moderate ratios of electric field strength to background pressure since an electron does not have sufficient energy to cause an ionization until it disperses into the tail of the energy distribution.

It was observed, in the recent random walk (RW) effort of reference 9, however, that relaxation times (thus number of steps) are inversely dependent on the coefficient of dispersion (second moment) of the energy exchange between the electrons and the electric field rather than the much smaller energy exchange between the electrons and background molecules. It was, in turn, demonstrated that the modern computer is capable of making detailed RW studies of the motion in a gaseous conductor with reasonable expenditures of computer time. Calculations for a typical set of conditions require about 5 to 15 minutes on a modern electronic computer.

The RW was applied to the electron motion in a weakly ionized helium gas in reference 9 over a wide range of E/p. (Symbols are defined in appendix A.) In the present study this effort is extended to include a magnetic field B perpendicular to the electric field. The ratio B/p is varied from low values where it has a negligible effect on the motion to high values where the electrons are closely tied to the magnetic field lines.

The ratio E/p was held constant at a value of 22.5 volt-meter per newton (30 V/cm-torr), which is high enough for appreciable occurrences of inelastic collisions, yet well below the range of electron runaway. Electron drift, diffusion, and Townsend first ionization coefficients are determined as well as mean energies, and velocity and energy distributions. Pertinent theory and its simplifying approximations are appraised.

ANALYSIS

Each test electron of a large sample is walked for predetermined macroscopic time intervals. Each such walk comprises a large number of steps. Each step includes an analytically determined trajectory terminated by an encounter with another particle. Time between collisions as well as the type of interaction and concomitant scattering angles are determined through selection of random numbers. The macroscopic time intervals are selected to suitably study the relaxation of an ensemble of electrons from an initial arbitrary, to a steady state, velocity distribution.

In the crossed field configuration of interest (fig. 1) both the electric field and magnetic field are constant in space and time. The background helium gas is assumed only weakly ionized so that interactions between charged particles can be neglected. The electrons are quite ineffective in heating the relatively heavy background atoms. Thus these atoms are essentially cold, or stationary, and the medium is a Lorentz gas (ref. 10). The time during a short range interaction, as between an electron and a neutral, is negligible for the gas densities of interest. Thus the effect of the electric and magnetic fields on the electron motion need be accounted for only during the free time t between collisions.

Electron Trajectories During Free Time

The conservation of momentum of an electron during the free time is

$$m \frac{d\vec{v}}{dt} = -e(\vec{E} + \vec{v} \times \vec{B})$$

where $e = 1.602 \times 10^{-19}$ coulomb. The solution to this equation (ref. 10) for the velocity components is

$$\left.\begin{aligned} v_x &= \left(v_{x,i} + \frac{E}{B}\right)\cos(\omega t) + v_{y,i}\sin(\omega t) - \frac{E}{B} \\ v_y &= v_{y,i}\cos(\omega t) - \left(v_{x,i} + \frac{E}{B}\right)\sin(\omega t) \\ v_z &= v_{z,i} \end{aligned}\right\} \quad (1)$$

and for the spacial coordinates is

$$\left.\begin{aligned} x &= x_i + \frac{1}{\omega}\left\{\left(v_{x,i} + \frac{E}{B}\right)\sin(\omega t) + v_{y,i}\left[1 - \cos(\omega t)\right] - \frac{\omega t E}{B}\right\} \\ y &= y_i + \frac{1}{\omega}\left\{v_{y,i}\sin(\omega t) - \left(v_{x,i} + \frac{E}{B}\right)\left[1 - \cos(\omega t)\right]\right\} \\ z &= z_i + v_{z,i}t \end{aligned}\right\} \quad (2)$$

where $\vec{v} = (v_{x,i}, v_{y,i}, v_{z,i})$ at $t = 0$ and, for the crossed field configuration of figure 1, $\vec{E} = (0, -E, 0)$ and $\vec{B}$ $(0, 0, B)$. The subscript i denotes conditions at the start of the free trajectory, which are the conditions resulting from the preceding collision. Equations (1) and (2) describe trochoidal electron trajectories having cyclotron motion of frequency $\omega = -eB/m$ and drift velocity equal to $\vec{E} \times \vec{B}/B^2$.

Free Time Between Collisions

Descriptive integrals and approximate solutions. - During each step of a random walk, a free time t is selected at random from a distribution of free times $f(t)$. In its general form this distribution can be expressed (ref. 9) as

$$f(t) = nQ_a v \exp\left(-\int_0^t nQ_a v\, dt'\right) = \tau F_t\left(\frac{t}{\tau}\right) \quad (3)$$

where Q_a is the sum of the total cross sections of all the various type interactions between the test electrons and background atoms.

The mean free time between collisions is

$$\tau = \int_0^\infty tf(t)dt = \int_0^\infty tnQ_a v \exp\left(-\int_0^t nQ_a v\, dt'\right) dt$$

which reduces to (ref. 9)

$$\tau = \int_0^\infty \exp\left(-\int_0^t nQ_a v\, dt'\right) dt \tag{4}$$

by use of integration of parts and L'Hospital's rule.

The interaction energy of an electron (or ion) with a neutral atom is sometimes approximated by the polarization potential (ref. 8) which varies as the inverse fourth power of the distance between centers of the two interacting particles. This is the case of the Maxwell molecule (refs. 10 and 11) for which $Q_{el}v$ is a constant, Q_{el} being the total elastic scattering cross section. It is thus plausible that $Q_a v$ is close to being constant, as assumed in reference 12, for example.

A plot of the experimentally obtained value of $Q_a v$ for helium (refs. 13 and 14) against ϵ is shown in figure 2. A value of $Q_a v$ of 7.8×10^{-14} cubic meter per second is within 5 percent of this curve for $5 \leq \epsilon \leq 80$ eV; however, for $\epsilon << 5$ eV this is a poor approximation.

When $Q_a v$ is constant over the time period, equation (4) reduces to

$$\tau = \left(nQ_{a,i}v_i\right)^{-1} \tag{5}$$

and a distribution of free times becomes simply

$$F_t\left(\frac{t}{\tau}\right) = \exp\left(\frac{-t}{\tau}\right) \tag{6}$$

The free time random number correspondence (ref. 15)

$$\int_0^{R_t} dR_t' = \int_0^{t/\tau} F_t\left(\frac{t'}{\tau}\right) d\left(\frac{t'}{\tau}\right) \tag{7}$$

integrates in this case to

$$\frac{t}{\tau} = \ln\left(\frac{1}{R_t}\right) \tag{8}$$

The random numbers are drawn from a set of numbers uniformly distributed over the interval from 0 to 1. Routines to provide such numbers are available in most computer libraries.

Numerical evaluation of free time integrals. - It was found in the study of reference 9 that the components of drift velocity and diffusion coefficient parallel to the electric field, $v_{D,y}$ and D_y, were the most sensitive of the calculated electron transport coefficients to approximations of equations (3) and (4). Use of equation (5) gave the desired accuracy of $v_{D,y}$ and D_y only for $E/p < 7.5$ volt-meter per newton (10 V/cm-torr). The electron energy distributions and remaining electron transport coefficients were found sensitive to the approximation of equation (5) for E/p values of 45 volt-meter per newton and greater. Results were found to be much less affected by the approximation of equation (6).

The presence of a magnetic field restrains electron motion and, as shown later, lowers the effective E/p making it less than 22.5 volt-meter per newton (30 V/cm-torr) for the present study. Nevertheless the suitability of equations (5) and (6) for use in the present study is further appraised. Typical results showing the influence of the crossed field configuration on the mean free time parameter $\Upsilon = nQ_{a,i}v_i\tau$ and on the distribution of free times about the mean free time are shown in figures 3 and 4, respectively.

The solid lines of figure 3 present Υ values obtained by numerically integrating equation (4) with use of equations (1) and the data of figure 2.

Empirical curves, shown by the dashed lines, were fit to the numerical results for use in the computer program. The empirical relations used are given by equations (33) and (34) in table I. Figure 3(a) shows the effect of $\cos\theta_i$ and ϵ_i on Υ at $\varphi_i = 0$ and $B/p = 7.1\times10^{-5}$ weber per newton whereas figures 10(b) and (c) show the influence of φ on Υ at various ϵ_i and $\cos\theta_i$. Figure 10(d) shows the effect of B/p on Υ at various ϵ_i and at the polar angle π where the effect is most pronounced. The parameter Υ was found to differ appreciably from 1 only when ϵ_i is less than 5 eV and B/p is

much less than 10^{-4} weber per newton. The electron energy distributions, to be presented later, show that only a relatively small number of electrons lie in the low energy range less than 1 eV.

A value of t/τ is determined by selection of a random number R_t for each step of a random walk. The corresponding value of τ is then obtained by use of

$$\tau = \frac{\Upsilon}{nQ_{a,i}v_i}$$

The empirical relation between t/τ and R_t, which approximates numerical solution of equations (7) and (3), and which is used in the computer program, is given in equation (35) of table I. The distribution of t/τ, obtained by drawing values of R_t from a uniformly distributed set and then using this empirical relation, is shown in figure 4 by the data symbols. These symbols represent tallies of 3×10^4 discrete values of t/τ. The dash-dot lines represent the distributions obtained directly by numerical integration of equation (3).

The approximate distribution of equation (6) is given by the solid lines. The largest differences between equation (6) and the exact numerical results of equation (3) is in the vicinity of an ϵ_i value of 0.5. Equation (6) provides a good approximation to equation (3) for $\epsilon_i \geq 5$ eV.

Type of Interaction

At the end of each free time period a random number R_Q is drawn to determine the type of interaction.

It can be seen from the data of references 16 and 17 that the number of excited helium atoms is negligible for background gas temperatures of interest. The electron affinity for neutral helium atoms is less than zero, thus the formation of negative atoms is also negligible (ref. 18). The interactions of interest are, therefore, between free electrons and ground state atoms, and

$$Q_a = Q_{el} + Q_{ex} + Q_{ion} \tag{9}$$

The correspondence between the type of interaction and R_Q can then be as follows. When

$$R_Q \leq \frac{Q_{el}}{Q_a}$$

the electron undergoes an elastic collision. When

$$\frac{Q_{el}}{Q_a} < R_Q \leq \frac{Q_{el} + Q_{ex}}{Q_a}$$

the calculation for an excitation is made, and when

$$\frac{Q_{el} + Q_{ex}}{Q_a} < R_Q$$

an ionization is assumed.

The integral cross sections used in the analyses are shown in figure 5. The ionization cross section is from the experimental investigation of reference 19. The excitation cross section is the sum of the cross sections for excitation from the ground state to the next seven energy levels in both the singlet and triplet spectral series of helium (ref. 17). The cross section for elastic collisions was obtained by subtracting Q_{ex} and Q_{ion} from Q_a.

Scattering Angles

Once the type of interaction is known, the scattering angle can be determined. The relation between differential scattering cross section $\sigma(\epsilon, \chi)$ and uniformly distributed random number R_χ is

$$R_\chi = \frac{\int_0^\chi \sigma(\epsilon, \chi') \sin \chi' \, d\chi'}{\int_0^\pi \sigma(\epsilon, \chi') \sin \chi' \, d\chi'}$$

where χ is the scattering angle in local spherical coordinates.

The experimental differential scattering cross section data of references 20, 13, and 21 were used for elastic encounters (fig. 6(a)) and that of references 20, 22, and 23 for inelastic encounters (fig. 6(b)).

The inelastic data are primarily the cross section for excitation of the most probable state (2^1P) from the ground state (1^1S). Little differential scattering data to other states is available. The data of reference 24 show essentially the same distribution of

scattering angle for excitation to the 2^1P, 3^1P, or 4^1P states. The data of figure 6(b) are also used to represent ionization events.

The recent experimental results of reference 23 show a steeper rise of $\sigma(\chi)$ with decrease of χ and a slightly lesser effect of ϵ than the results of references 20 and 22. Two sets of curves were therefore used to find the effect of these differences on electron transport coefficients. The data symbols in figure 6 represent tallies of 3×10^4 values of χ obtained from drawing R_χ and using relations (36) to (38) of table I.

Azimuthal angle α is uniformly distributed; thus

$$\alpha = 2\pi R_\alpha \tag{10}$$

Energy Losses

The energy lost from an electron $\Delta\epsilon$ and given to an atom during an elastic interaction is (ref. 10)

$$\Delta\epsilon = \frac{2m}{M}\epsilon(1 - \cos\chi) \tag{11}$$

For excitations the average $\Delta\epsilon$ for scattering to the first seven states in the singlet and triplet series is used. This average was found equal to 21.9±0.1 eV over the range of interest (ref. 9).

The minimum energy lost in an ionization event is the potential energy, 24.46 eV. It is assumed that the remaining kinetic energy is evenly divided between the test and the liberated electron. Thus, $\epsilon_i = (\epsilon - 24.46)/2$ after an ionization event. The effect of various ionization energy loss assumptions on RW results are studied in reference 9.

Coordinate Systems

The transformation to spherical coordinates at the end of each free time period is

$$
\left.
\begin{aligned}
v &= \sqrt{v_x^2 + v_y^2 + v_z^2} \\
\theta &= \cos^{-1}\left(\frac{v_y}{v}\right) \\
\varphi &= \tan^{-1}\left(\frac{v_x}{v_z}\right)
\end{aligned}
\right\} \qquad (12)
$$

whereas the transformation from the scattering coordinates back to spherical laboratory coordinates at the end of each collision calculation is

$$
\left.
\begin{aligned}
v_i &= \sqrt{v^2 - \frac{2\,\Delta\epsilon}{m}} \\
\theta_i &= \cos^{-1}\left(\cos\chi\cos\theta + \sin\chi\sin\theta\cos\alpha\right) \\
\varphi_i &= \varphi + \frac{\cos^{-1}\left(\cos\chi - \cos\theta\cos\theta_i\right)}{\sin\theta\sin\theta_i}
\end{aligned}
\right\} \qquad (13)
$$

In summary, to perform a random walk for this weakly ionized plasma, four random numbers are drawn for each step. The first, R_t, to determine the ratio of free to mean free time, then R_Q to determine the type of encounter; finally R_χ and R_α to determine the scattering and azimuthal angles. The trajectories during the free time are determined by analytical solution to the equations of motion, whereas the collisional interactions are based on experimental data.

As an initial condition at the start of the very first free path for each test electron, an isotropic distribution in angle θ_i was assumed. The electron energy at the start of each walk was set equal to a constant value close to the expected average energy at the steady state. The steady state, or terminal conditions were found in preliminary calculations to be independent of the initial condition selected.

Determination of Macroscopic Quantities at Steady State Conditions

During the walk of each test electron, the time T equal to the accumulative free times of the walk, is monitored. At prescribed time periods, $T = T_1, T_2, \ldots, T_j$, the energy distribution of all the test electrons is determined. This is obtained by tallying the numbers of test electrons which have energy within the various equal increments of the range of ϵ. The time period was increased logarithmically until there were no observable changes in the energy distribution $F_\epsilon(\epsilon)$ with time, indicating that steady state conditions are reached.

After such a terminal state is reached, the drift velocities can be obtained from

$$\left.\begin{aligned} v_{D,x} &= \frac{\sum (x - x_i)}{\sum t} = \frac{\sum (x - x_i)}{A(T_j - T_{j-1})} \\ \text{and} \\ v_{D,y} &= \frac{\sum (y - y_i)}{A(T_j - T_{j-1})} \end{aligned}\right\} \qquad (14)$$

where the subscript j denotes the j^{th} time period, A is the number of test electrons, and the summations are over the free times of the A electrons between the j and $j-1$ time periods.

In like manner the various components of the diffusion coefficient are obtained from the second moments of distance during the free time periods as

$$\left.\begin{aligned} D_x &= \frac{1}{6} \frac{\sum (x - x_i)^2}{A(T_j - T_{j-1})} \\ D_y &= \frac{1}{6} \frac{\sum (y - y_i)^2}{A(T_j - T_{j-1})} \\ D_z &= \frac{1}{6} \frac{\sum (z - z_i)^2}{A(T_j - T_{j-1})} \end{aligned}\right\} \qquad (15)$$

The number of ionizations are also recorded during the time periods so that the Townsend ionization coefficient α_T can be obtained from

$$\alpha_T = \frac{\sum \text{number ionization events}}{\sum (y - y_i)} \tag{16}$$

Mean energy $\overline{\epsilon}$ is obtained from

$$\overline{\epsilon} = \int_0^\infty \epsilon F_\epsilon(\epsilon) d\epsilon \tag{17}$$

The walks of at least 1000 test electrons were determined for each B/p and physical model of particle behavior considered, from which the macroscopic quantities of equations (14) to (17) were obtained.

RESULTS AND DISCUSSION

Electron Energy and Velocity Distributions

The relaxation of the electron energy distributions from delta functions to terminal steady state conditions is shown in figure 7 for a wide range of B/p values. The time parameter tp and average number of collisions experienced per test particle in relaxing to the various intermediate distributions are also listed.

The values of these variables for relaxation to terminal conditions compare well with those obtained by use of the following theoretical relations based on the energy exchange criterion of reference 9:

$$N_\epsilon = 3\left(\frac{\overline{\epsilon} Q_a \frac{n}{p}}{e \frac{E}{p}}\right)^2 \left[1 + (\omega\tau)^2\right] \tag{18}$$

and

$$t_\epsilon p = 3\left(\frac{\bar{\epsilon} Q_a}{e\,\frac{E}{p}}\right)^2 \frac{\left[1 + (\omega\tau)^2\right]\frac{n}{p}}{Q_a v_i} \tag{19}$$

where n/p is the conventional ratio of number density to pressure at 0° C, equal to 2.65×10^{20} newton^{-1} meter^{-1} (3.54×10^{16} cm^{-3} torr^{-1}) and $\omega\tau$ is the Hall parameter. This theory is based on the second moment of the energy exchange between the electrons and the electric field. The extension to include a magnetic field for the case of interest is given in appendix B. Note that the magnetic field serves only to reduce the E/p ratio by $\sqrt{1 + (\omega\tau)^2}$. The product $p\sqrt{1 + (\omega\tau)^2}$ may be considered an effective pressure (ref. 25).

In relaxing to the steady state, the peaked distributions spread out very rapidly at first. At high B/p there is a shifting of the energy distribution toward lower energies near the final stages of the relaxation. This is apparently due to the decreased net amount of energy the electrons receive from the electric field as B is increased (see eqs. (B3) and (B4) of appendix B) which, at steady state conditions, must balance the electron energy lost in collisions. At a B/p of 2×10^{-4} weber per newton, the number of collisions for relaxation to a terminal distribution is about five times that required at $B = 0$. Beyond a B/p of 2×10^{-4} weber per newton, the required number of steps per walk and thus computer time rapidly increased to excessive values.

Steady state energy distributions were found to be independent of the energy ϵ_o of the initial delta function distributions. That the average number of steps per walk required for relaxation was also quite independent of ϵ_o is illustrated in figure 8.

Marginal distributions of the three rectangular components of random velocity, defined as

$$\left.\begin{aligned} F_{x,r} &= \int_{-\infty}^{\infty}\int_{-\infty}^{\infty} f(v_{x,r} v_{y,r} v_{z,r}) dv_{y,r}\, dv_{z,r} \\ F_{y,r} &= \int_{-\infty}^{\infty}\int_{-\infty}^{\infty} f(v_{x,r} v_{y,r} v_{z,r}) dv_{x,r}\, dv_{z,r} \end{aligned}\right\} \tag{20}$$

and

$$F_{z,r} = \int_{-\infty}^{\infty}\int_{-\infty}^{\infty} f(v_{x,r} v_{y,r} v_{z,r}) dv_{y,r}\, dv_{z,r}$$

are plotted in figure 9 at a high and a low B/p. The distributions are close to Maxwellian (referenced to $\overline{\epsilon}_r = 3\ k\Theta/2$) at all B/p investigated. This agrees with the theory of reference 10 for $Q_{el}v$ equal to a constant.

Mean Random Energy and Transport Coefficients in Helium

The mean random electron energy and Townsend's first ionization coefficient at steady state conditions are plotted against B/p in figure 10. The dashed lines were obtained by reading $\overline{\epsilon}_r$ and α_T/p from the B = 0 curves of reference 9 at effective ratios of electric field to pressure equal to $E\Big/\left[p\sqrt{1 + (\omega\tau)^2}\right]$. The effect of B/p on $\overline{\epsilon}_r$ and α_T/p is quite well accounted for by such a procedure, which is consistent with the findings of reference 25 for hydrogen. The mean energy predicted by reference 10, however, is about a factor of 10 too high.

Two simplifying assumptions, often used theoretically, are also appraised: the use of an isotropic distribution of scattering angle χ and the assumption that $Q_a v$ is a constant (constant mean free time between collisions). These assumptions changed the mean energy less than 10 percent; tending to lower $\overline{\epsilon}_r$ at low B/p and raise $\overline{\epsilon}_r$ at high B/p. The α_T/p results were also changed less than 10 percent except at the highest B/p value.

The α_T/p values appear to have the most data scatter of the RW results. This is due to the relatively small number of ionizing encounters.

Drift velocities in the $\vec{E}$ and $\vec{E} \times \vec{B}$ directions are plotted in figure 11. The effect of B/p is shown to be quite well predicted by the theoretical relations (ref. 10)

$$v_{D,x} = v_{D,x}(B = 0)\ \frac{\omega\tau}{\sqrt{1 + (\omega\tau)^2}} \tag{21}$$

and

$$v_{D,y} = \frac{v_{D,y}(B = 0)}{\sqrt{1 + (\omega\tau)^2}} \tag{22}$$

which are based on the assumption that $Q_a v$ is a constant. Drift velocity at B = 0 was obtained from reference 9.

The use of the simplifying assumption that $Q_a v$ is constant had very little effect on the RW determined drift, the changes being less than 10 percent. This assumption

raised $v_{D,x}$ slightly. The isotropic scattering approximation also consistently lowered $v_{D,y}$ and raised $v_{D,x}$. This is most pronounced at low B/p and is due to the fact that the isotropic approximation destroys the persistence of velocity trend exhibited in the differential scattering cross section data (fig. 5).

The three cartesian components of diffusion coefficient are plotted in figure 12. Theory based on $Q_a v$ equal to a constant yields (ref. 26)

$$pD_x = pD_x(B = 0) \frac{\omega\tau}{1 + (\omega\tau)^2} \tag{23}$$

$$pD_y = \frac{pD_y(B = 0)}{1 + (\omega\tau)^2} \tag{24}$$

and

$$pD_z = pD_z(B = 0) \tag{25}$$

Values of diffusion coefficient at B = 0 were obtained from reference 9. These relations slightly underestimate the decrease of D_x and D_y with increase of B/p as shown by the line comprised of long dashes. This discrepancy is more apparent for the z component and is due to the decrease of $\overline{\epsilon}$ with B/p (see fig. 9(a)) as yet unaccounted for.

Diffusion coefficient is proportional to v^2; thus multiplying the theoretical values in equations (24) and (25) by $\overline{\epsilon}_r / \overline{\epsilon}_r(B = 0)$ reduced the analytical results to close agreement with the basic RW calculations for all three components. This is shown by the line comprised of alternating long and short dashes in figure 11.

Results were very insensitive to the isotropic scattering assumption as well as to the use of $Q_a v$ set equal to a constant. Results agree to within the amount of scatter in the data, estimated to be less than 5 percent.

In general, holding Q_a constant (equal to 7.8×10^{-14} m^3/sec) over the whole range of ϵ to which the electrons have access has a fairly small influence on transport coefficients. The simplification of holding $Q_a v$ constant (equal to $Q_{a,i} v_i$) only during any given free time period, and thus permitting the use of equations (5) and (6), should be of even smaller consequence. The effect on the transport coefficients of using equation (5) in place of equation (4) is observable at lower B/p, however very little effect is observable at the intermediate values of B/p (7×10^{-5} Wb/N). The change of results due

to replacing equation (3) with equation (6) is within the data scatter even at the lowest B/p studied.

In much the same manner, the incorporation of the relatively small difference of results between the differential scattering cross sections of reference 23 with references 20 and 22 was found to have a negligible effect compared to the replacement of the cross sections of figure 6 with an isotropic distribution of scattering angle.

CONCLUSIONS

The present random walk study made over a wide range of magnetic field strengths leads to the following conclusions regarding electron motion in helium at an E/p of 22.5 volt-meter per newton (30 V/cm-torr) where E is the electric field strength and p is pressure at 0° C:

1. The restraining effect that the magnetic field has on the electron motion causes an increase in the relaxation time and corresponding number of steps (free time periods) for an assembly of electrons to reach a terminal steady state distribution. This trend can be predicted by use of an effective ratio of electric field to background pressure, equal to $E/p\sqrt{1 + (\omega\tau)^2}$ (where ω and τ^{-1} are the cyclotron and collision frequency, respectively), in the relaxation equation for magnetic field strength B = 0. The amount of computer time to perform random walks sufficient to simulate the electron motion of interest is within reason for B/p values up to at least 2.25×10^{-4} weber per newton (300 G/torr).

2. Distribution of random velocity was found to be close to the Maxwellian form theoretically predicted by Chapman and Cowling for the case of the collision frequency parameter $Q_a v$ equal to a constant. This theory, however, predicts a mean random energy, about which the particles are distributed, which is a factor of about 10 too high at E/p = 22.5 volt-meter per newton (30 V/cm-torr).

3. The use of the effective pressure concept enables determination of the dependence of mean random energy and Townsend ionization coefficient on B/p from knowing only their dependence on E/p at B = 0.

4. Existing theory (see Chapman and Cowling) was quite satisfactory in predicting drift motion as well as the x and y components of diffusion. The drop off of the z component of diffusion coefficient pD_z with increase of B/p could be accounted for through the fall off of mean random energy $\overline{\epsilon}_r$ with increase of B/p.

5. The simplifying assumption of constant mean free time was appraised by incorporating a constant value of absorption cross section times electron velocity $Q_a v = 7.8\times10^{-14}$ cubic meter per second in the random walk (RW). Results in general were quite insensitive to this restriction and changed less than 10 percent except for the

value of α_T/p (where α_T is the Townsend ionization coefficient) at the highest B/p (equal to 2.25×10^{-4} Wb/N). The assumption of an isotropic distribution of scattering angle was studied in like manner. The largest influence of this simplification was in the lowing of the y component of drift velocity due to the elimination of the persistance of velocity in the negative E direction during scattering.

Lewis Research Center,
National Aeronautics and Space Administration,
Cleveland, Ohio, November 11, 1971,
112-02.

APPENDIX A

SYMBOLS

[The International System of Units (SI) can be used throughout the equations. Numerical results are often presented in other units as well for ease of comparison with previous investigations.]

A	number of test electrons or walks
a	constant defined in table I
B	magnetic field strength
C	constant defined in table I
D	diffusion coefficient
E	electric field strength
e	absolute value of electrostatic charge of an electron, 1.602×10^{-19} C
F	distribution function
f	distribution function
M	mass of a helium molecule, 6.695×10^{-27} kg
m	mass of an electron, 9.108×10^{-31} kg
N	average number of steps per walk
n	number density at 0° C
p	pressure at 0° C
Q	integral cross section
R	random number
r	variable defined in table I
S	variable defined in table I
T	time at which data are recorded
t	time
v	velocity
v_{ref}	reference random velocity, $\sqrt{2\overline{\epsilon}_r/m}$
x	Cartesian coordinate antiparallel to $\vec{E}\times\vec{B}$

y Cartesian coordinate antiparallel to $\vec{E}$

z Cartesian coordinate parallel to $\vec{B}$

α azimuthal scattering angle (see fig. 1)

α_T Towsend ionization coefficient

β variable in table I

ϵ electron energy

Θ temperature

θ polar angle

σ differential cross section

τ mean free time between collisions

Υ mean free time parameter equal to ratio of mean free time to mean free time for constant $Q_{a,i}v_i$

φ azimuthal angle in x,y plane

χ scattering angle

ω electron cyclotron frequency

Subscripts:

a absorption

D drift

el elastic

ex electron excitation

i at the start of the free time period

ion ionization

o condition at start of walk

Q denotes a random number drawn to determine type of collisional interaction

r random

t time

x x component

y y component

z z component

α denotes a random number drawn to determine azimuthal angle

ϵ relaxation to terminal distribution based on energy exchange

φ pertains to azimuthal angle in x,y plane

χ denotes a random number drawn to determine scattering angle

APPENDIX B

THEORETICAL APPROXIMATION OF RELAXATION TIME

The energy relaxation time of reference 27 is defined as

$$t_\epsilon = \frac{\tau \overline{\epsilon^2}}{\overline{(\Delta\epsilon)^2}} \tag{B1}$$

In like manner the average number of collisions per test electron for relaxation to a steady state is

$$N_\epsilon = \frac{\overline{\epsilon^2}}{\overline{(\Delta\epsilon)^2}} \tag{B2}$$

It was found in reference 9 that this criterion gives good comparison with RW results if the energy exchange $\Delta\epsilon$ is based on the interaction of the electrons and the electric field.

Considerable energy is usually exchanged between the electron and the field during a free time period. That is, the absolute value of $\Delta\epsilon$ is usually large. When accounting for algebraic sign, however, the much smaller average net amount of energy given to the electrons by the field just balances the energy transfer from the electrons to the cold neutrals at steady state conditions. An average based on the second moment of $\Delta\epsilon$ yields the square of the gross electron field energy exchange. Relative to the magnitude of this average, the drift energy and energy loss to neutrals (first moments) can be neglected within the accuracy desired for relaxation time estimates.

The effort of reference 9 is extended herein to include a magnetic field. For the cross field configuration of interest

$$\overline{(\Delta\epsilon)^2} = e^2E^2\,\overline{(\Delta y)^2} \tag{B3}$$

where

$$\Delta y = \frac{1}{\omega}\left\{v_{y,i}\sin(\omega t) - \left(v_{x,i} + \frac{E}{B}\right)\left[1 - \cos(\omega t)\right]\right\}$$

Since Δy is a function of $v_{x,i}$, $v_{y,i}$, and t,

$$\overline{(\Delta y)^2} = \int_0^\infty \int_{-\infty}^\infty \int_{-\infty}^\infty (\Delta y)^2 f_v(v_{x,i}, v_{y,i}) f_t(t) dv_{x,i}\, dv_{y,i}\, dt$$

where within desired accuracy

$$f_t(t) = \frac{1}{\tau} e^{-t/\tau}$$

as previously discussed.

Due to the large angle scattering in α and χ, the $v_{x,i}$ and $v_{y,i}$ are essentially uncorrelated, thus

$$f_v(v_{x,i} v_{y,i}) \simeq f_{v,x}(v_{x,i}) f_{v,y}(v_{y,i})$$

If drift velocities are neglected, $f_{v,x}$ and $f_{v,y}$ are even functions of $v_{x,i}$ and $v_{y,i}$, respectively. Since the drift motion $\overline{E} \times \overline{B}/B^2$ can also be neglected for purposes at hand, the first moments and, therefore, also products of first moments of Δy are zero. Thus

$$\overline{(\Delta y)^2} = \frac{1}{\omega^2 \tau} \int_0^\infty \int_{-\infty}^\infty v_{y,i}^2 \sin^2(\omega t) f_{v,y}(v_{y,i}) e^{-t/\tau}\, dv_{y,i}\, dt$$

$$+ \frac{1}{\omega^2 \tau} \int_0^\infty \int_{-\infty}^\infty v_{x,i}^2 \left[1 - 2\cos(\omega t) + \cos^2(\omega t)\right] f_{v,x}(v_{x,i}) e^{-t/\tau}\, dv_{x,i}\, dt$$

This integrates to

$$\overline{(\Delta y)^2} = \frac{\overline{2v_i^2} \tau^2}{3\left[1 + (\omega\tau)^2\right]} \tag{B4}$$

where it is assumed that

$$\overline{v_{x,i}^2} = \overline{v_{y,i}^2} = \frac{1}{3}\overline{v_i^2}$$

for the near isotropic distribution of interest.

It can be further approximated that

$$2\tau^2\overline{v_i^2} = l^2 = \frac{1}{n^2Q_a^2} \tag{B5}$$

as on page 19 of reference 26, where l is the mean free path. Thus, using equations (B3), (B4), and (B5) in equation (B2) yields

$$N_\epsilon = 3\left(\frac{\overline{\epsilon} n Q_a}{eE}\right)^2 \left[1 + (\omega\tau)^2\right] \tag{18}$$

Using equations (5), (18), and (B2) in equation (B1) gives

$$t_\epsilon p = 3\left(\frac{\overline{\epsilon} Q_a}{e\frac{E}{p}}\right)^2 \frac{\left(\frac{n}{p}\right)\left[1 + (\omega\tau)^2\right]}{Q_a v_i}$$

Let, for helium, $Q_a v_i = 0.78\times10^{-13}$ cubic meter per second; then

$$t_\epsilon p = 10^{34}\left(\frac{\overline{\epsilon} Q_a}{e\frac{E}{p}}\right)^2 \left[1 + (\omega\tau)^2\right], \text{ N-sec/m}^2 \tag{19}$$

REFERENCES

1. Loeb, Leonard B.: Basic Processes of Gaseous Electronics. Univ. of California Press, 1955.
2. Von Engle, A. H.: Ionized Gases. Second ed., Clarendon Press, Oxford, 1965.
3. Crookes, William: On the Illumination of Lines of Molecular Pressure, and the Trajectory of Molecules. Phil. Trans., vol. 1, 1879, pp. 135-164.
4. Pearson, Karl: The Problems of the Random Walk. Nature, vol. 72, no. 1865, July 27, 1905, p. 294.
5. Chandrasekhar, S.: Stochastic Problems in Physics and Astronomy. Rev. Mod. Phys., vol. 15, no. 1, Jan. 1943, pp. 1-89.
6. DeHoog, F. J.: A Random Walk to a Simple Stationary Electron Energy Distribution. Physica, vol. 40, 1968, pp. 139-149.
7. Yarnold, G. D.: The Energies of Uniformly Accelerated Particles in a Gas. Phil. Mag., vol. 36, no. 254, Mar. 1945, pp. 185-200.
8. Wannier, Gregory H.: Motion of Gaseous Ions in Strong Electric Fields. Bell Syst. Tech. J., vol. 32, no. 1, Jan. 1953, pp. 170-254.
9. Englert, Gerald W.: Random Walk Theory of Elastic and Inelastic Time Dependent Collisional Processes in an Electric Field. Zeit. f. Naturforschung, vol. 26A, no. 5, May 1971, pp. 836-848.
10. Chapman, Sydney; and Cowling, T. G.: The Mathematical Theory of Non-Uniform Gases. Second ed., Cambridge University Press, 1952.
11. Vincenti, Walter G.; and Kruger, C. H.: Introduction to Physical Gas Dynamics. John Wiley & Sons, Inc., 1965.
12. Reder, Fritz H.; and Brown, Sanborn, C.: Energy Distribution Function of Electrons in Pure Helium. Phys. Rev., vol. 95, no. 4, Aug. 15, 1954, pp. 885-889.
13. Ramsauer, C.; and Kollath, R.: Angular Distribution in the Scattering of Slow Electrons by Gaseous Molecules. Annalen der Physik, Ser. 5, vol. 12, 1932, pp. 529-561.
14. Normand, C. E.: The Absorption Coefficient for Slow Electrons in Gases. Phys. Rev., vol. 35, no. 10, May 15, 1930, pp. 1217-1225.
15. Schreider, Yu. A., ed.: Method of Statistical Testing, Monte Carlo Method. Elsevier Publ. Co., 1964.
16. Sovie, Ronald J.; and Dugan, John V., Jr.: Effects of Metastable Atoms on Volume Ion Production in a Tenuous Helium Plasma. NASA TN D-3121, 1965.

17. Sovie, Ronald J.; and Klein, Barry M.: Volume Ion Production in a Tenuous Helium Plasma. NASA TN D-2324, 1964.

18. McDaniel, Earl W.: Collision Phenomena in Ionized Gases. John Wiley & Sons, Inc., 1964.

19. Smith, Philip T.: The Ionization of Helium, Neon, and Argon by Electron Impact. Phys. Rev., vol. 36, no. 8, Oct. 15, 1930, pp. 1293-1302.

20. Mohr, C. B. O.; and Nicoll, F. H.: Inelastic Electron Scattering in Gases. - I. Proc. Roy. Soc. (London), Ser. A, vol. 138, no. 834, Oct. 1, 1932, pp. 229-244.

21. Massey, H. S. W.; and Burhop, E. H. S.: Electronic and Ionic Impact Phenomena. Vol. 1. Second ed., Clarendon Press, Oxford, 1969.

22. Nicoll, F. H.; and Mohr, C. B. O.: The Inelastic Scattering of Slow Electrons in Gases. - III. Proc. Roy. Soc. (London), Ser. A, vol. 142, no. 846, Oct. 1, 1933, pp. 320-332.

23. Truhlar, Donald G.; Rice, James K.; Kuppermann, Aron; Trajmar, S.; and Cartwright, D. C.: Differential and Integral Cross Sections for Excitation of the 2^1P State of Helium by Electron Impact. Phys. Rev., vol. 1A, no. 3, Mar. 1970, pp. 778-802.

24. Mott, N. F.; and Massey, H. S. W.: The Theory of Atomic Collisions. Third ed., Clarendon Press, Oxford, 1965.

25. Blevin, H. A.; and Haydon, S. C.: The Townsend Ionization Coefficients in Crossed Electric and Magnetic Fields. Australian J. Phys., vol. 11, 1958, pp. 18-34.

26. Allis, W. P.: Motions of Ions and Electrons. Tech. Rep. 299, Massachusetts Inst. Tech. Res. Lab. Electronics, June 13, 1956.

27. Chandrasekhar, S.: The Time of Relaxation of Stallar Systems. I. Astrophys. J., vol. 93, 1941, pp. 285-304.

TABLE I. - EMPIRICAL CURVE FITS

Equation	Equation number	Plotted in figure -
$T = \begin{cases} 1.47 - 0.01\epsilon_i - \left(0.556 - 0.16\sqrt{\epsilon_i}\right)\left[2.5(1 + \cos\theta_i) + 0.05\epsilon_i^3\right]^{1/3} + \Delta T & \text{if } \epsilon_i > 0.325 \text{ eV} \\ 1.433\epsilon_i^{0.467}(1 - 0.7\epsilon_i \cos\theta_i) + \Delta T & \text{if } \epsilon_i \le 0.325 \text{ eV} \end{cases}$	(33)	3(a)
$\Delta T = 0.529\left(1 + \cos\theta_i\right)^{0.2} \exp - \left(1 + \cos\theta_i\right)^3\left[\sqrt{r^2 - 2.46} - \sqrt{r^2 - \left(\varphi_i - a\right)^2}\right]$	(34)	3(b) and 3(c)
where		
$r = 7.78 - 10\sqrt{\epsilon_i}\exp(-\epsilon_i) + \left\lvert\epsilon_i - 0.6\right\rvert^{3.5}$		
and		
$a = \begin{cases} \frac{\pi}{2} & \text{if } 0 \le \varphi_i \le \frac{3}{2}\pi \\ \frac{5}{2}\pi & \text{if } \frac{3\pi}{2} \le \varphi_i \le 2\pi \end{cases}$		
$\frac{t}{\tau} = \ln\left[\frac{1}{(1 - R_t)}\right] - \frac{0.35\,S}{\epsilon_i}\left[1 - \left\lvert\cos\left(\varphi - \frac{\pi}{2}\right)\right\rvert \sin\beta\right]$	(35)	4
where		
$S = \begin{cases} \sqrt{\frac{R_t}{(1 - R_t)}} & \text{if } \cos\theta_i < 0 \\ \left[\frac{R_t}{(1 - R_t)}\right]^R & \text{if } \cos\theta_i \ge 0 \end{cases}$		
$\beta = \begin{cases} \pi\left[(2 - \cos\theta_i)R_t - 1.1\cos\theta_i - 0.1\right] & \text{if } \cos\theta_i < 0 \\ 2\pi(R_t - C) & \text{if } \cos\theta_i \ge 0 \end{cases}$		
and		
$C = \begin{cases} 0 & \text{if } R \le 0.4 \\ 0.1 & \text{if } R > 0.4 \end{cases}$		
$\chi = \cos^{-1}\left(1 - 2R_x^y\right)$	(36)	6(a)
where $y = 1 + \left(\frac{\epsilon_i}{30}\right)^a$ and $a = 1.7$		
$\chi = \begin{cases} \cos^{-1}\left(1 - 2R_x^y\right) \text{ where } y = 1 + \left(\frac{\epsilon}{30}\right)^a \text{ with } a = 1 & \text{if } \epsilon_i \le 60 \text{ eV} \\ \frac{120}{\epsilon_i}\sin^{-1}\left(R_x^{1.55}\right) & \text{if } \epsilon_i > 60 \text{ eV} \end{cases}$	(37)	6(b)
$\chi = \begin{cases} \frac{4}{\sqrt{\epsilon_i}}\sin^{-1}\left(R_x^{1.55}\right) & \text{if } \epsilon_i \le 44 \text{ eV} \\ 0.6\sin^{-1}\left(R_x^{1.55}\right) & \text{if } \epsilon_i > 44 \text{ eV} \end{cases}$	(38)	6(b)

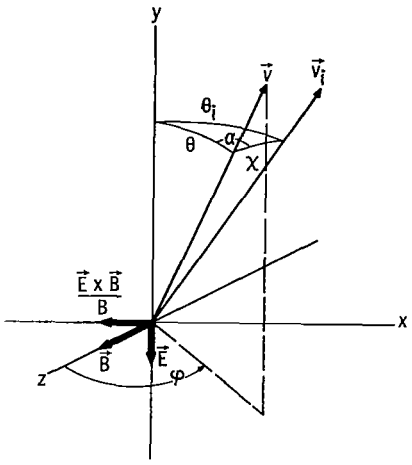

Figure 1. - Coordinate system.

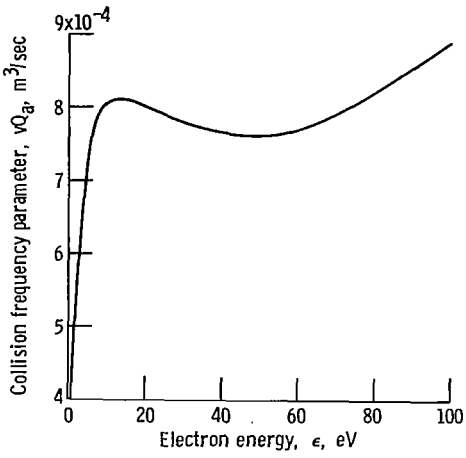

Figure 2. - Collision frequency parameter νQ_a in helium plotted against electron energy ϵ.

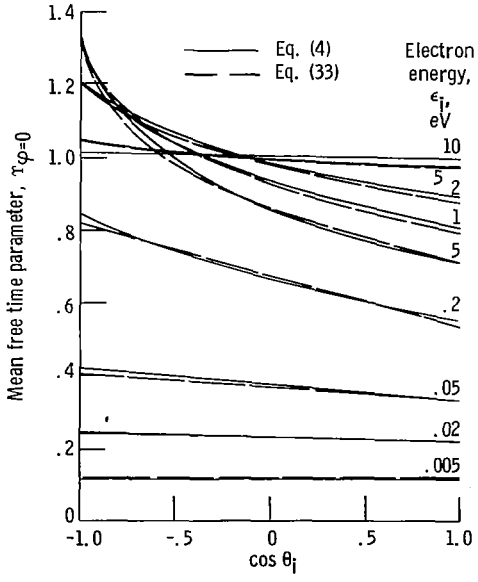

(a) Influence of electron energy ϵ_i and polar angle θ_i when azimuthal angle $\varphi_i = 0$ and ratio of magnetic field strength to background pressure $B/p = 7.1 \times 10^{-5}$ weber per newton (95 G/torr).

Figure 3. - Effect of conditions at start of electron trajectories on mean free time parameter τ.

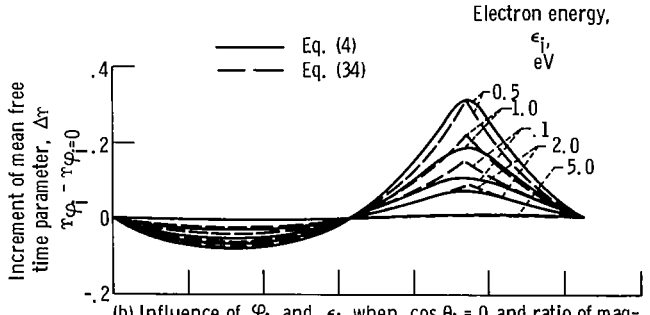

(b) Influence of φ_i and ϵ_i when $\cos\theta_i = 0$ and ratio of magnetic field strength to background pressure $B/p = 7.1 \times 10^{-5}$ weber per newton (95 G/torr).

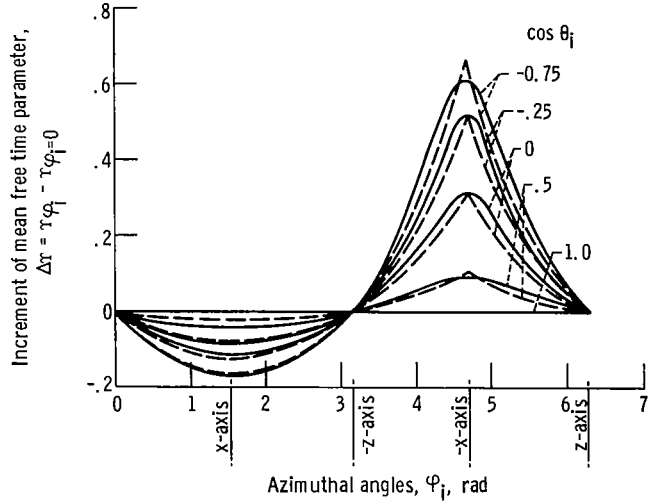

(c) Influence of φ_i and $\cos\theta_i$ when $\epsilon_i = 0.5$ eV and ratio of magnetic field strength to background pressure $B/p = 7.1 \times 10^{-5}$ weber per newton (95 G/torr).

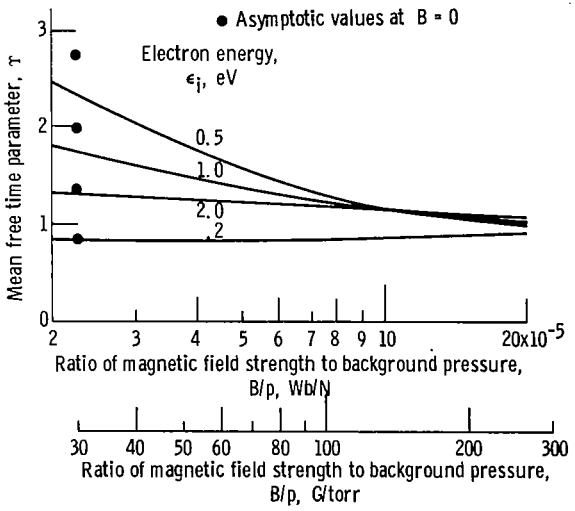

(d) Influence of B/p and ϵ_i when azimuthal angle $\varphi_i = \pi/2$ radians and $\cos\theta_i = -1$.

Figure 3. - Concluded.

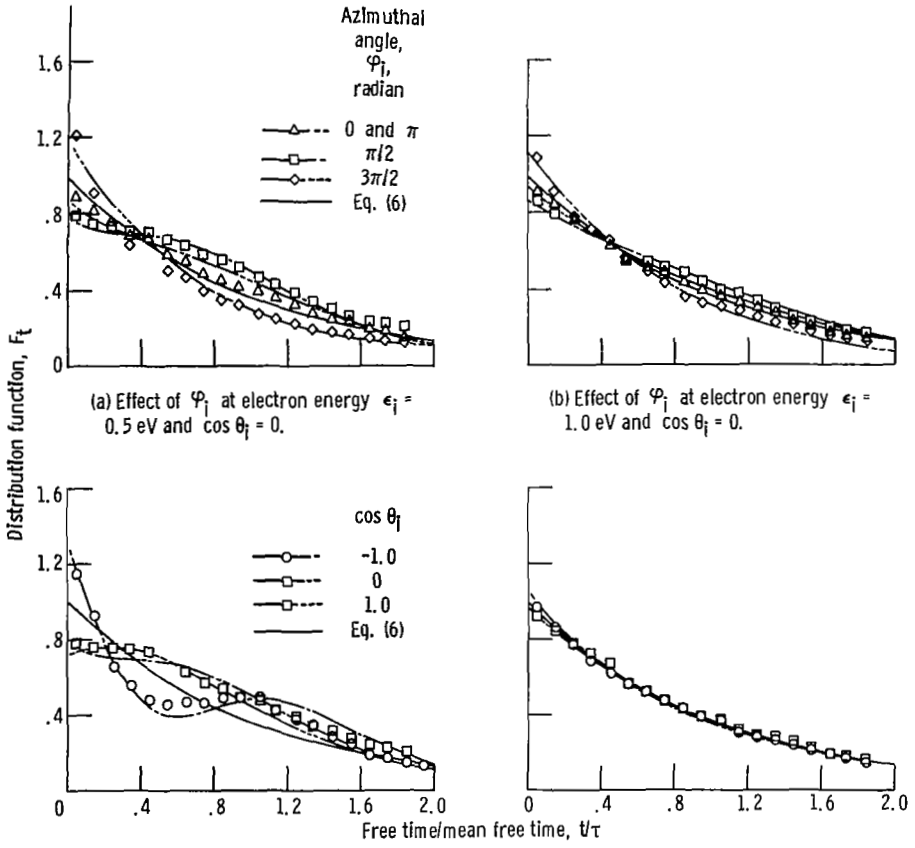

(a) Effect of φ_i at electron energy ϵ_i = 0.5 eV and $\cos\theta_i = 0$.

(b) Effect of φ_i at electron energy ϵ_i = 1.0 eV and $\cos\theta_i = 0$.

(c) Effect of θ_i at ϵ_i = 0.5 eV and azimuthal angle $\varphi_i = \pi/2$ radians.

(d) Effect of θ_i at ϵ_i = 5.0 eV and azimuthal angle $\varphi_i = \pi/2$ radians.

Figure 4. - Effect of conditions at start of electron trajectories on distribution F_t of free time t about mean free time τ. Ratio of magnetic field strength to background pressure $B/p = 7.1 \times 10^{-5}$ weber per newton (95 G/torr). Symbols denote tallies of distributions of random numbers obtained by using equation (35). Dash-dot lines denote numerical integration of equation (3).

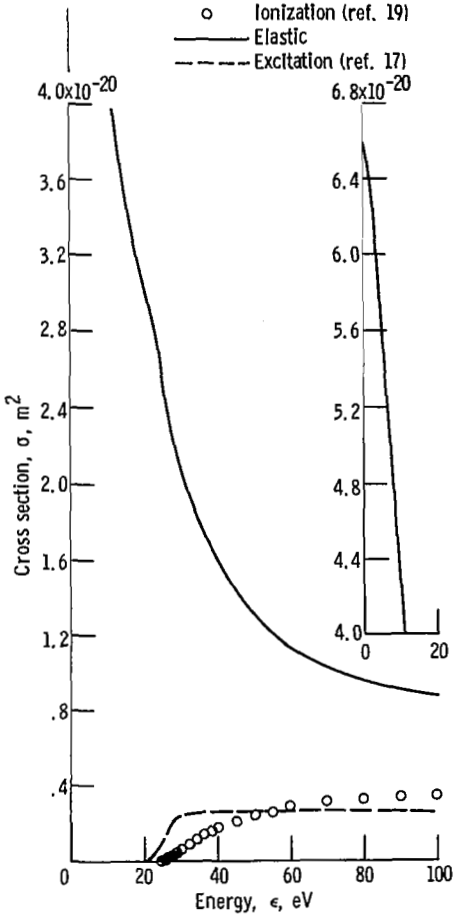

Figure 5. - Cross sections for interaction of electrons with helium. Elastic cross sections obtained from absorption cross sections of references 13 and 14 minus excitation and ionization cross sections.

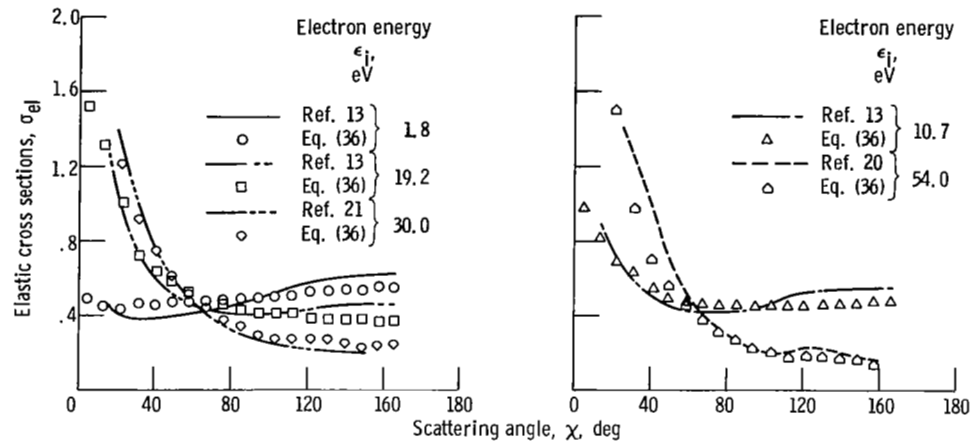

(a) Elastic scattering.

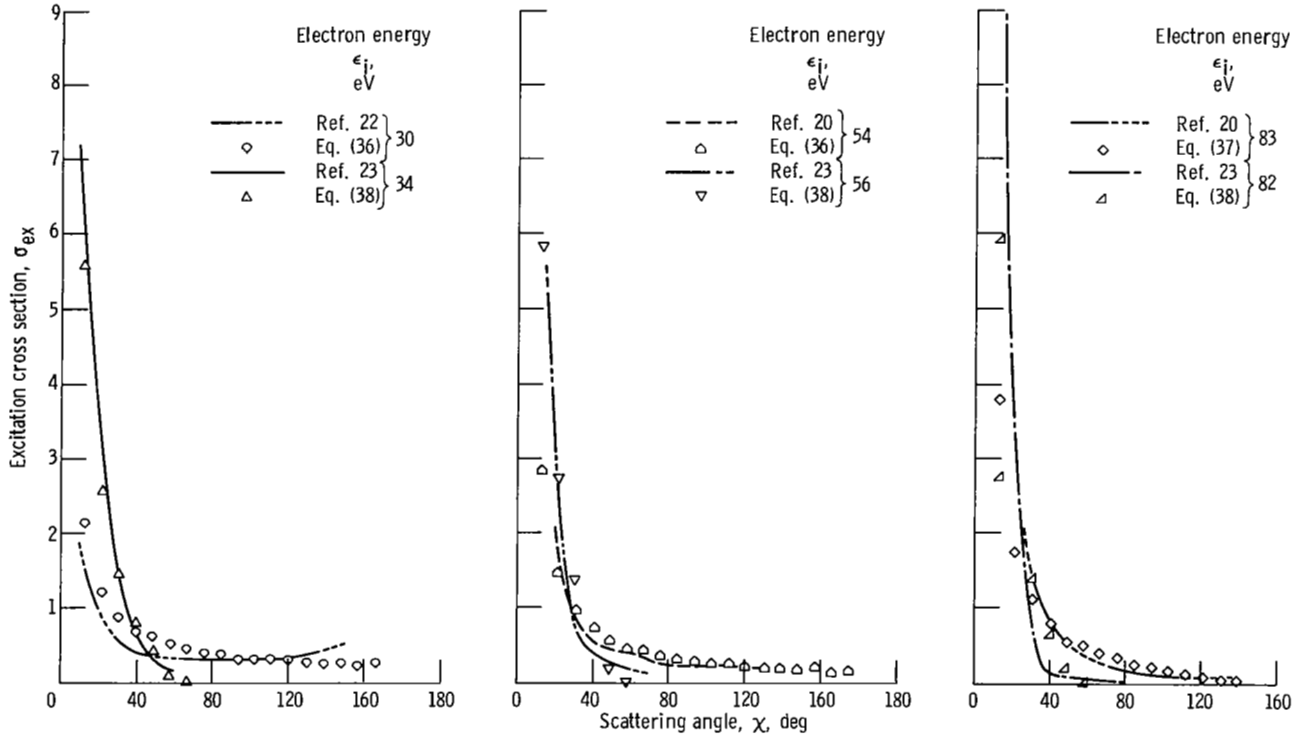

(b) Inelastic scattering from ground to 2^1P state.

Figure 6. - Differential scattering cross sections σ versus scattering angle χ. Lines are for experimental data and symbols are for tallies of distributions of random numbers R_χ obtained with use of equations (36) to (38).

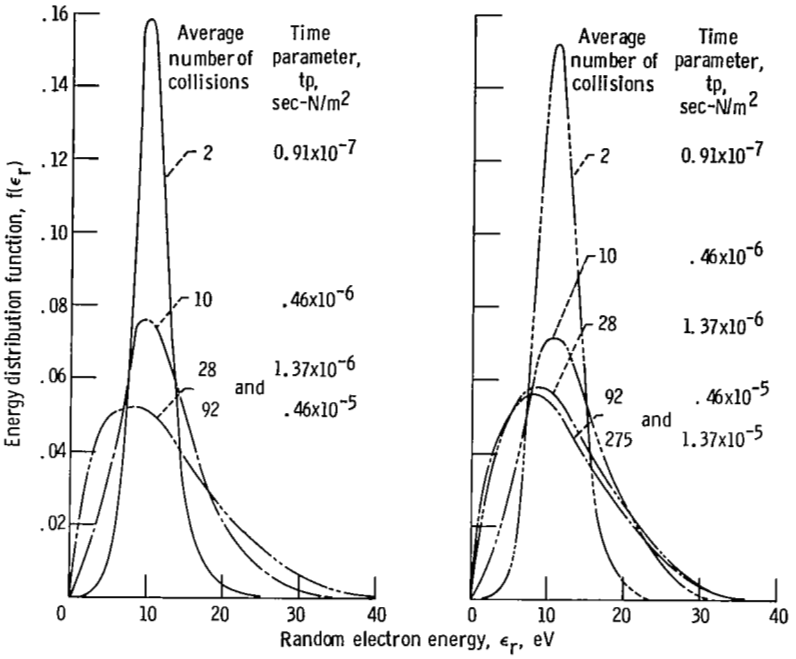

(a) Magnetic field strength B = 0; average number of collision predicted by equation (18) N_ϵ = 93; corresponding time predicted by equation (19) $t_\epsilon p$ = 0.45x10^{-5}.

(b) Ratio of magnetic field strength to background pressure B/p = 2.25x10^{-5} weber per newton (30 G/torr); average number of collisions predicted by equation (18) N_ϵ = 97; corresponding time predicted by equation (19) $t_\epsilon p$ = 0.47x10^{-5}.

Figure 7. - Electron energy distribution at various times of relaxation from an initial delta function. Time t is multiplied by pressure p of helium referenced to 0^0 C. E/p = 22.5 volt-meter per newton (30 V/cm-torr).

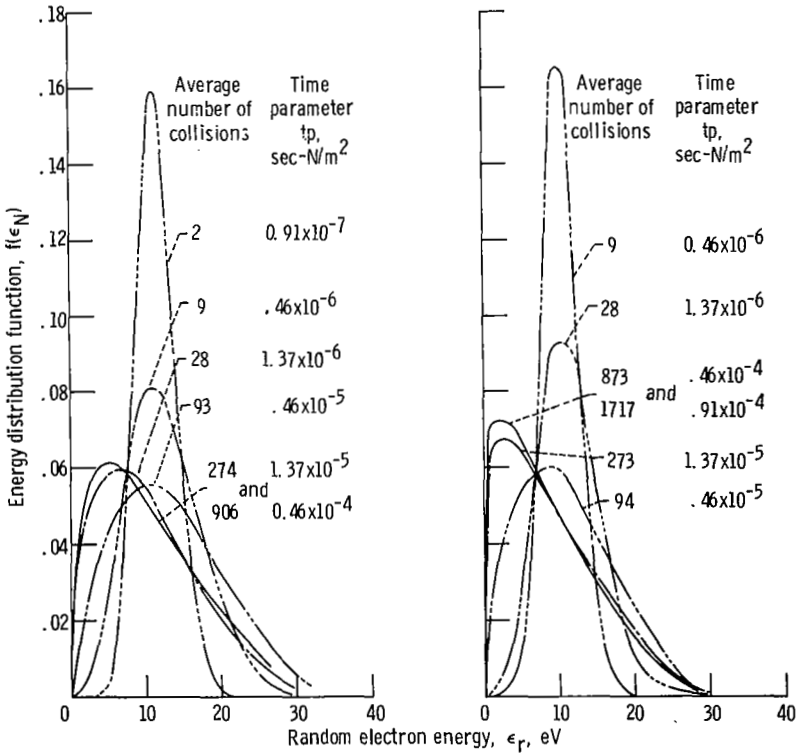

(c) Ratio of magnetic field strength to background pressure $B/p = 0.71 \times 10^{-4}$ weber per newton (95 G/torr); average number of collisions predicted by equation (18) $N_\epsilon = 117$; corresponding time predicted by equation (19) $t_\epsilon p = 0.56 \times 10^{-5}$.

(d) Ratio of magnetic field strength to background pressure $B/p = 2.25 \times 10^{-4}$ weber per newton (300 G/torr); average number of collisions predicted by equation (18) $N_\epsilon = 318$; corresponding time predicted by equation (19) $t_\epsilon p = 0.15 \times 10^{-4}$.

Figure 7. - Concluded.

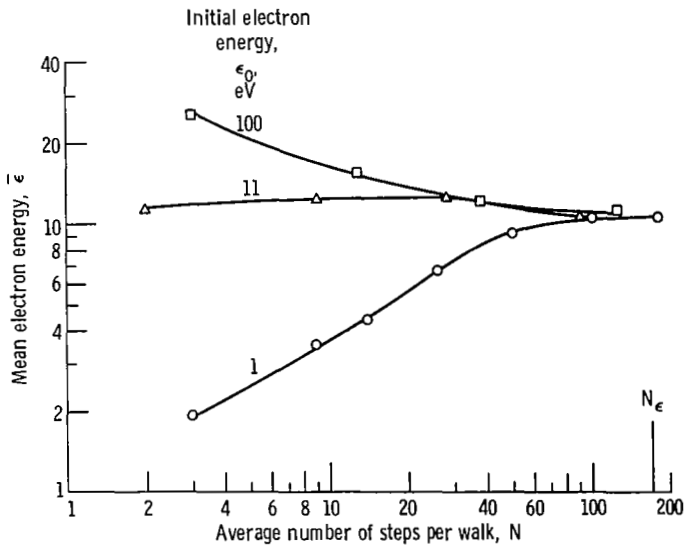

Figure 8. - Influence of initial electron energy ϵ_0 on mean electron energy ϵ versus average number of collisions per walk N. The theoretical value N_ϵ for relaxation to terminal conditions is from equation (18). Ratio of magnetic field strength to background pressure $B/p = 2.25 \times 10^{-5}$ weber per newton (30 G/torr).

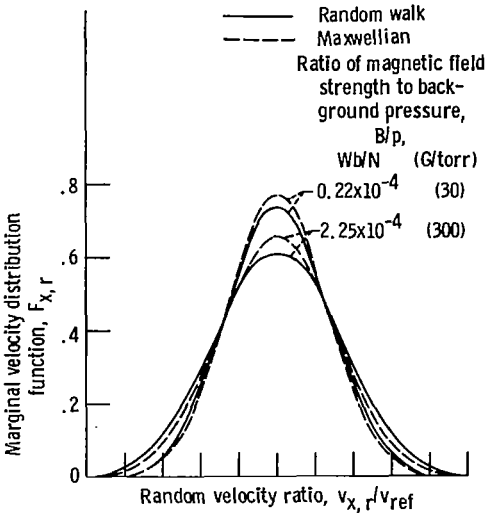

(a) x Component of random velocity.

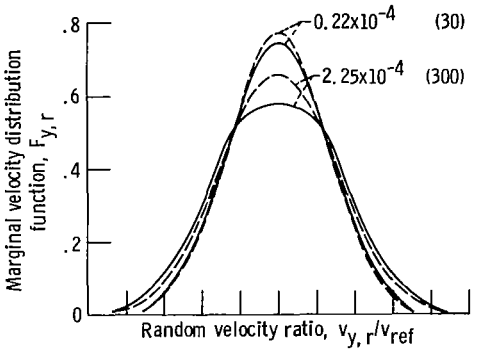

(b) y Component of random velocity.

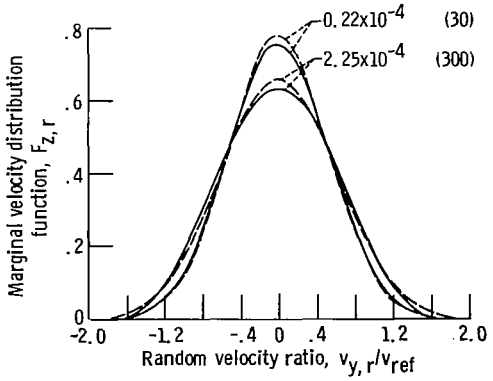

(c) z Component of random velocity.

Figure 9. - Electron marginal velocity distributions in helium. E/p = 22.5 volt-meter per newton (30 V/cm-torr).

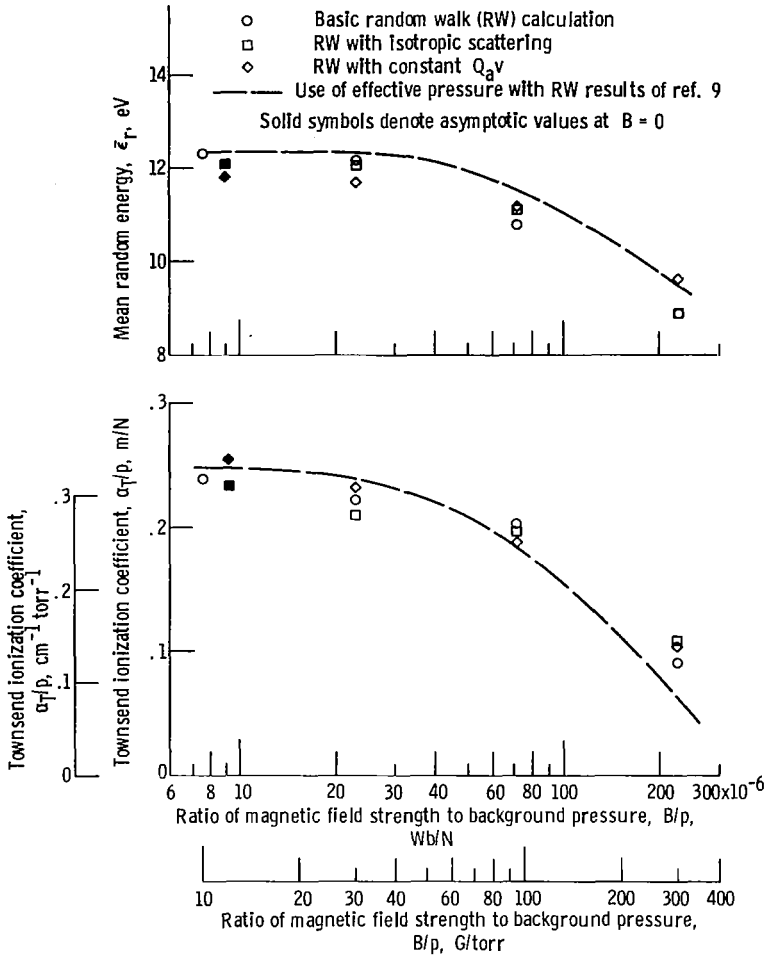

Figure 10. - Effect of magnetic field on mean random electron energy and on Townsend first ionization coefficient divided by helium pressure referenced to 0° C.

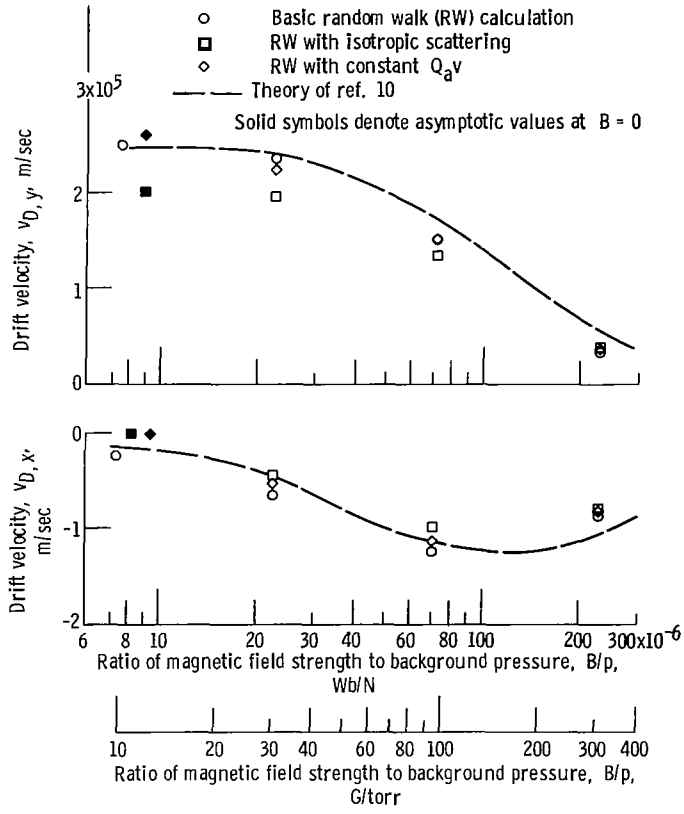

Figure 11. - Effect of magnetic field on drift velocities.

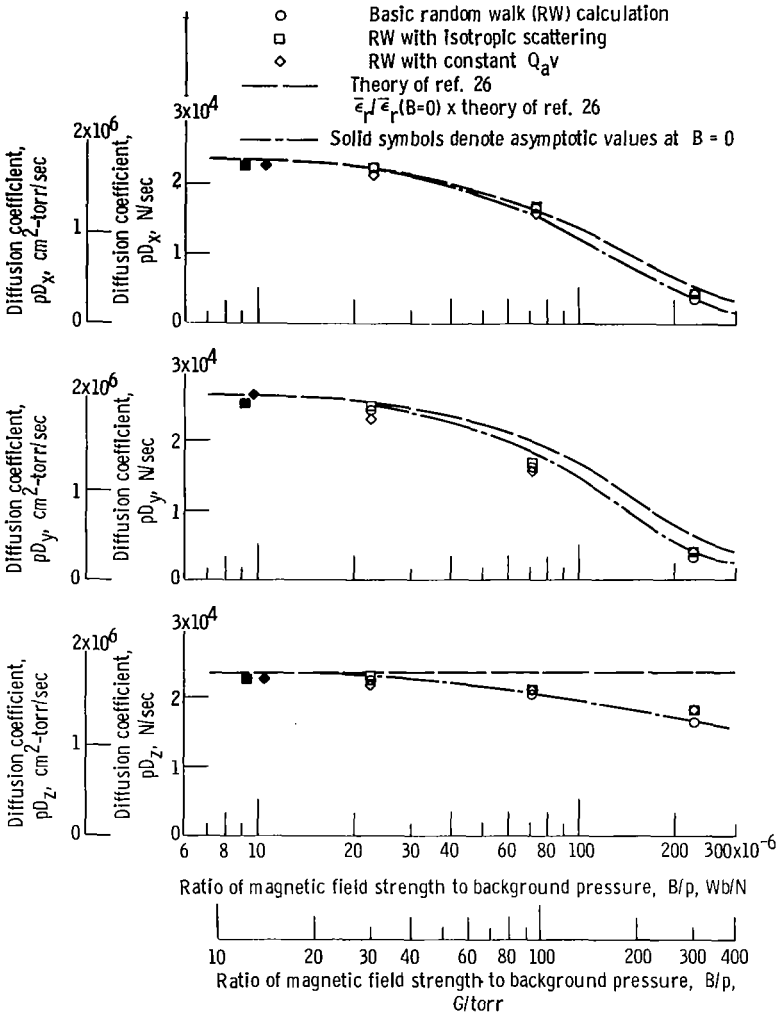

Figure 12. -Effect of magnetic field on diffusion coefficients multiplied by pressure of helium referenced to 0° C.